Acta Crystallographica Section D
Biological Crystallography
ISSN 0907-4449

Comparison of the refined crystal structures of wild-type (1.34 Å) flavodoxin from *Desulfovibrio vulgaris* and the S35C mutant (1.44 Å) at 100 K

Roberto Artali,[a] Gabriella Bombieri,[a]* Fiorella Meneghetti,[a] Gianfranco Gilardi,[b] Sheila J. Sadeghi,[b] Davide Cavazzini[c] and Gian Luigi Rossi[c]

[a]Institute of Pharmaceutical Chemistry, University of Milano, Italy, [b]Department of Biochemistry, Imperial College, London, England, and [c]Department of Biochemistry and Molecular Biology, University of Parma, Italy

Correspondence e-mail: gabriella.bombieri@unimi.it

Received 27 March 2002
Accepted 9 July 2002

Engineered flavodoxins in which a surface residue has been replaced by an exposed cysteine are useful modules to link multi-domain redox proteins obtained by gene fusion to electrode surfaces. In the present work, the crystal structure of the S35C mutant of *Desulfovibrio vulgaris* flavodoxin in the oxidized state has been determined and compared with a refined structure of the wild type (wt). The structure of wt flavodoxin (space group $P4_32_12$, unit-cell parameters $a = 50.52$, $b = 50.52$, $c = 138.59$ Å) at 1.34 Å resolution has been refined to $R = 0.16$ and $R_{\rm free} = 0.18$. The structure of the S35C mutant (space group $P4_32_12$, unit-cell parameters $a = 50.55$, $b = 50.55$, $c = 138.39$ Å) at 1.44 Å resolution has been refined to $R = 0.13$ and $R_{\rm free} = 0.16$. Data sets were collected with synchrotron radiation at 100 K. In the S35C mutant, the Cys35 thiol group points towards a hydrophobic region, whilst in the wt the Ser35 hydroxyl group points towards a more polar region. The solvent exposure of Cys35 is 43 Å^2, of which 8 Å^2 is for the sulfur. This is comparable to the exposure of 48 Å^2 found for the wt Ser35, where that of the hydroxyl oxygen is also 8 Å^2.

1. Introduction

Flavodoxins are small flavoproteins of 14–23 kDa containing flavin mononucleotide (FMN) as cofactor. They act as single-electron carriers in a variety of low-potential reactions in which the FMN cycles between the semiquinone and the hydroquinone states, while the oxidized state does not seem to participate in physiologically relevant redox reactions (Ludwig & Luschinsky, 1992). X-ray crystallography and NMR spectroscopy have been used to determine the structures of flavodoxins of different species (Hoover *et al.*, 1999). The first flavodoxin to be characterized was isolated from the cyanobacterium *Anacystis nidulans* (Smillie, 1965). Crystal structures have been determined for flavodoxin from *Clostridium* MP (Ludwig *et al.*, 1976), *Clostridium beijerinckii* (Ludwig *et al.*, 1997), *Desulfovibrio vulgaris*, with the FMN in its three oxidation states (Watt *et al.*, 1991), *Anacystis nidulans* (Smith *et al.*, 1983; Laudenbach *et al.*, 1987; Drennan *et al.*, 1999), *Megasphaera elsdenii* (van Mierlo *et al.*, 1990), *Chondrus crispus* (Fukuyama *et al.*, 1992), *Anabaena* 7120 (Burkhart *et al.*, 1995), *Escherichia coli* (Hoover & Ludwig, 1997), *Desulfovibrio desulfuricans* (Romero *et al.*, 1996) and *Helicobacter pylori* (Freigang *et al.*, 2002).

Flavodoxins are classified in two groups according to their molecular masses: 'long-chain' (169–176 residues) and 'short-chain' (138–147 residues) flavodoxins. Both groups belong to the class of α/β proteins, in which the central five-stranded parallel sheet lies between helices. The short-chain flavodoxin from *D. vulgaris* has been used together with cytochromes c_{553} and P450 BM3 as a 'module' to generate a multi-domain redox

protein for exploitation in bioelectrochemistry (Gilardi *et al.*, 2002; Sadeghi, Meharenna *et al.*, 2000; Sadeghi, Valetti *et al.*, 2000; Sadeghi *et al.*, 1999). This has been achieved with the molecular Lego approach, which proposes generation of artificial redox chains by linking well characterized redox proteins either by gene fusion or by an engineered disulfide bridge. For the latter, the presence of a unique surface cysteine is required at a specific position. Although wt flavodoxin contains four cysteines, none is exposed (Watt *et al.*, 1991) and available to form either intra- or intermolecular disulfide bridges (Valetti *et al.*, 1998). Therefore, one surface-exposed residue, namely Ser35, was mutated to cysteine on the basis of its solvent exposure. As the role of flavodoxin in the gene-fused multi-domain complex with cytochromes is to provide a link to the electrode surfaces *via* the engineered cysteine, the mutant S35C is expected to exhibit minimal disruption of the native structure and to have a solvent exposure of the engineered sulfydryl group of Cys35 comparable to that of the wt Ser35.

The principal aim of the present study is to compare the molecular model derived from synchrotron data of wt flavodoxin with that of the S35C mutant.

2. Results and discussion

The structure of the S35C *D. vulgaris* flavodoxin mutant in the oxidized state, as well as that of the wt protein, was determined from data collected at 100 K using synchrotron radiation. The two structures were determined at resolutions of 1.34 and 1.44 Å, respectively. A ribbon representation of their structure is shown in Fig. 1. The structure shows the five-stranded parallel β-sheet and, as for other flavodoxins, the two α-helices that flank each side of the β-sheet. The analysis of the secondary structure shows that the three-dimensional structures of the wt and S35C mutant are essentially superimposable. Small changes in the intra- and intermolecular contacts of the mutant with respect to the wt protein were observed. As is known from the published structure of wt flavodoxin, FMN interacts with the protein through hydrogen bonds as well as van der Waals and stacking interactions (Watt *et al.*, 1991). Many of these interactions involve backbone atoms of the protein. The isoalloxazine ring is sandwiched between the aromatic rings of the side chains of Trp60 and Tyr98 and is approximately coplanar with Tyr98 in both structures.

Figure 1
Structure of wt *D. vulgaris* flavodoxin showing FMN and the mutation site (Ser35).

Three segments of the protein interact with FMN and contribute to the binding of the prosthetic group: the phosphate-binding loop (10–15) and the sequences 56–62 ('loop 60') and 95–102 ('loop 100'). The latter contains the residues that are in direct contact with the isoalloxazine ring and are known to influence the reactivity and redox properties of the bound flavin. FMN shows the usual L shape, where the shorter arm, the isoalloxazine ring, has its terminal part oriented towards the protein surface. This facilitates solvent interactions and electron exchange with redox partners. The longer arm, the ribityl-phosphate, is also at the surface, with the ribityl partly exposed to solvent and the phosphate near the surface but buried by its hydrogen-bonding partners.

The network of hydrogen bonding between the FMN and the protein provides stability to the folding of the molecule. A comparison of hydrogen bonds in the wt and S35C mutant is shown in Fig. 2 (*LIGPLOT*; Wallace *et al.*, 1995). The hydrogen bonds were calculated with *HBPLUS* (McDonald & Thornton, 1994), where the lower limit fixed for the angles is 130° and the higher limit for the distance between the calculated H-atom position and the acceptor is 2.5 Å. The 'loop 60' conformation favours the interaction of Asp62 N with O(4) of the flavin ring in both wt and S35C. The N(5) of the isoalloxazine ring, which is involved in redox reactions (Watt *et al.*, 1991), only makes contacts with NH of Asp62 in both wt and the S35C mutant (3.39 and 3.36 Å, respectively).

The 'loop 100' makes important interactions with the isoalloxazine moiety. Residues 95, 100 and 102 form backbone hydrogen bonds to the atoms N(3) and O(2) in both wt and S35C. An Asp95 N interaction with N(1) is present only in S35C.

The phosphate loop 'loop 10', with the sequence Ser10–Thr15, adopts a conformation in which Gly13 has torsional angles that are the same for the wt and the S35C (the respective values are $\psi = 98$ and 97°; $\varphi = -4$ and −3°). Strong interactions between the phosphate O atoms and the NH groups of the loop are suggested by the short O···N distances in the range 2.5–2.9 Å for wt and S35C. In addition, the distance between Ser58 O^{γ} and OP3 of the FMN moiety is 2.83 and 2.67 Å in wt and S35C, respectively. It is interesting to note that in S35C the orientation of the cysteine thiol group is different to that of the serine hydroxyl group in wt. This finding may be explained by the hydrophobic character of cysteine in proteins. As shown in a recent study (Nagano *et al.*, 1999), cysteine residues are preferentially located in hydrophobic clusters with methionine, tryptophan and tyrosine, and tend to be separated from serine and threonine, which are located in polar clusters. In keeping with this observation, in the structure of the S35C mutant we find that the Cys35 thiol group points towards a hydrophobic region in the direction of Tyr8 (Cys35—SH torsion angle −169°), while in the wt structure the Ser35 hydroxyl group (torsion angle −66°)

points towards a more hydrophilic region flanked by Ala23 and Val33 as shown in Fig. 3. A comparison with the crystal structure of the *D. vulgaris* apoflavodoxin–riboflavin complex (Walsh *et al.*, 1998) shows that in this case the torsion angle Ser35—OH is −179°, pointing toward Tyr8 as for S35C mutant. A parallel to this behaviour is found when comparing the conformation of this residue in the two mutants Y98H and Y98W of *D. vulgaris* flavodoxin (Reynolds *et al.*, 2001). While in Y98H the torsion angle is −75° in agreement with our results for wt, in Y98W at 1.5 Å resolution a double conformation has been found, with a torsion angle of −74° in one conformer and −171° in the second conformer. We can therefore assume a small energy difference between the two conformations, the substitution of serine with cysteine favouring one conformer respective to the other one.

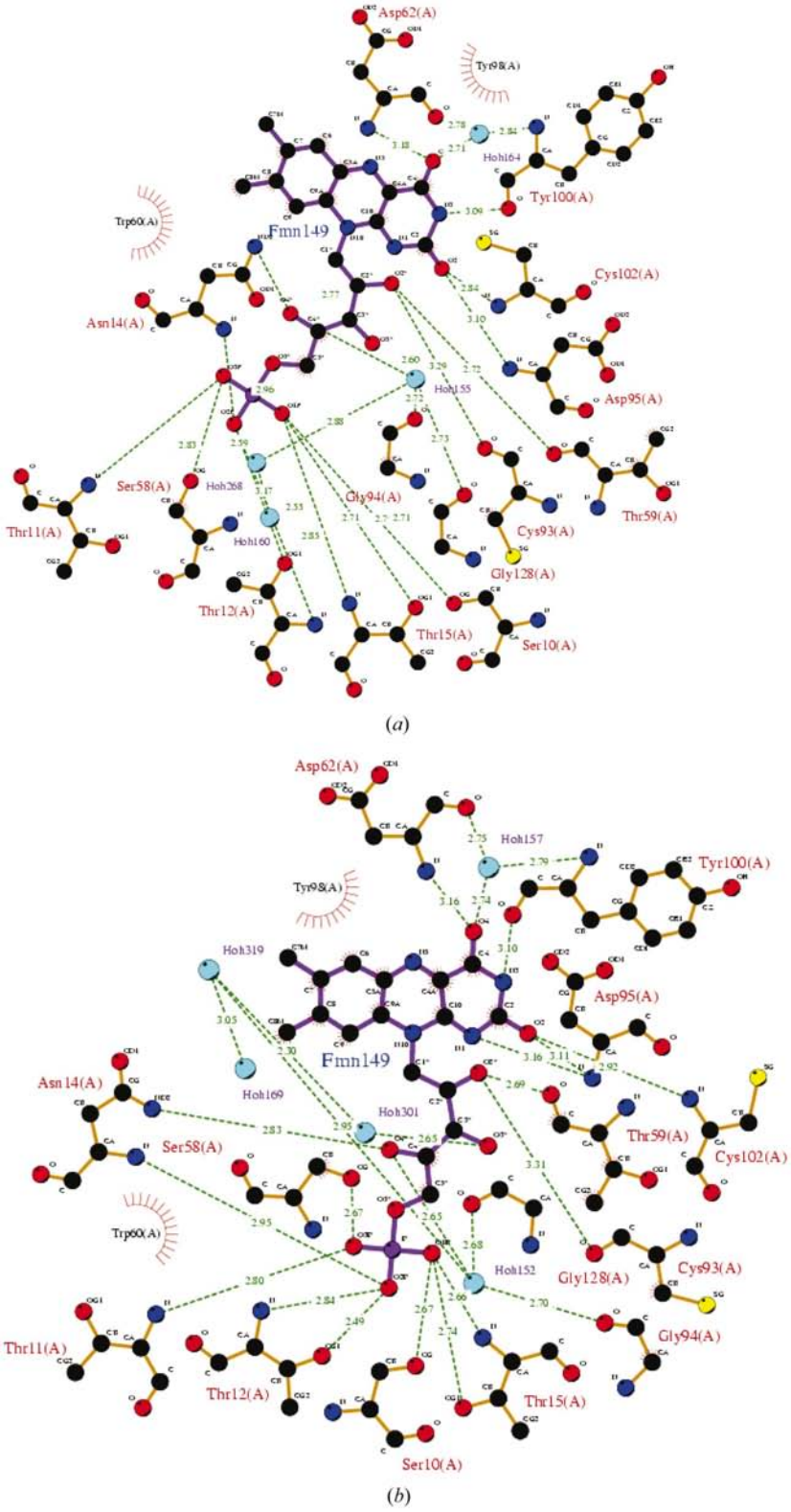

Figure 2
LIGPLOT representation of hydrogen bonding at the flavin-binding site in (*a*) wt and (*b*) S35C flavodoxin.

The exposure to solvent of Ser35 (wt) and Cys35 have been calculated using the Connolly algorithm with a probe radius of 1.4 Å (Table 1). The surface accessibility of Cys35 was found to be comparable to that of Ser35 of wt: the total areas are 43 and 48 Å^2, respectively, of which 8 Å^2 pertain to either the S atom or the hydroxyl O atom. These values show that the mutation does not cause significant changes to the native structure.

The average r.m.s. deviation calculated between the wt model at 1.9 Å resolution (low temperature; Watt *et al.*, 1991) and the present determination (1.34 Å resolution) is 0.24 Å for main-chain atoms and 0.53 Å for side-chain atoms. The largest deviation occurs at Glu42, but no significant effects have been detected on either intra- or intermolecular contacts. Considering the conformation of the Arg24 side chain, which shows the largest deviation between the models at room and low temperature (Watt *et al.*, 1991), we note that at higher resolution at low temperature (100 K) the hydrogen bonds involving N$^{\varepsilon}$ are oriented differently than reported previously. They involve both the carboxylic side-chain groups O$^{\delta1}$ and O$^{\delta2}$ of Asp28; in the structure at 1.9 Å resolution (Watt *et al.*, 1991), the contacts are only with Asp28 O$^{\delta2}$ (low temperature), while Arg24 NH$_2$ only makes a loose contact with Asp28 O$^{\delta2}$. Fig. 4 shows the plot of the r.m.s. differences for each residue obtained by superimposition of the crystallographic structures of wt at 1.34 Å resolution and the S35C mutant. The similarity of the two structures is reflected by r.m.s.d. values of 0.14 and 0.16 Å between corresponding C$^{\alpha}$ and main-chain atoms, respectively. The largest r.m.s. differences arise from residues located around the mutation site. A comparison of the wt and S35C structures indicates that the substitution of Ser35 has not perturbed the overall confor-

mation, but the protein segment '30–50' around the mutation site presents the highest structure deviation. A significant difference in the orientation of Tyr98 is also observed: in wt flavodoxin it is almost coplanar with the isoalloxazine ring (about 9° between the respective planes) as reported previously (Watt *et al.*, 1991), while in the S35C mutant the corresponding angle is 23°. In the absence of significant intramolecular contacts in either structure, this could be simply related to the relative degree of freedom of the Tyr98 ring, owing to its position almost at the surface of the protein. Several conformations of 'loop 60' have also been found in *D. vulgaris* mutants (Tyr98, Gly61; Reynolds *et al.*, 2001) as expected if a small energy difference exists between them. The isoalloxazine ring in S35C is less buried in the polypeptide chain than it is in wt, with an angle between the flavin ring and Trp60 of 166° in the mutant and 146° in wt. The high-resolution data collected for wt and the S35C mutant allow the analysis of a detailed $2F_o - F_c$ electron-density map as shown in Fig. 5, in which the non-H-atom positions of the flavin ring are clearly shown. The isoalloxazine ring is not planar: both the wt and the mutant structures show a bow in the FMN. The angle between the best mean planes of the dimethylbenzene and pyrimidine wings (calculated with *SHELX*97) is 8.8 (3)° for wt and 11.0 (3)° for S35C, with a mean deviation from planarity for the whole isoalloxazine moiety of 0.1 Å in both. The mean of the distribution of bending angles in different oxidized flavoprotein structures (Lennon *et al.*, 1999) is 7.0 ± 5.2° and the results obtained for the *D. vulgaris* wt and S35C mutant are within the calculated range.

Table 1
Selected values of the Connolly surface accessibility (Å^2).

Area	Contact	Re-entrant	Total
Cys35	15.0	28.5	43.5
Ser35	16.3	31.7	48.0
Cys35 S	0.7	7.4	8.1
Ser35 O	1.5	7.0	8.5

Table 2
Crystal data and refinement statistics.

λ used was 1 Å and T = 100 K. Values in parentheses refer to the last resolution shell.

	Wt	S35C
Molecular weight (Da)	15650	15666
Space group	$P4_32_12$	$P4_32_12$
Unit-cell parameters (Å)		
$a = b$	50.52	50.55
c	138.59	138.39
V (Å^3)	353719	353628
Resolution range (Å)	28.51–1.34 (1.42–1.34)	16.37–1.44 (1.52–1.44)
Reflections [$F > 4\sigma(F)$/all data]	33487/35789	27836/29127
Completeness (%)	94.4 (94.3)	95.3 (91.6)
Redundancy	4.6 (4.5)	3.8 (3.8)
R [$F > 4\sigma(F)$/all data]	0.158/0.160	0.134/0.136
R_{free} [$F > 4\sigma(F)$/all data]	0.180/0.181	0.156/0.158
Non-H atoms		
Protein	1102	1102
FMN	31	31
Solvent (HOH)	185	174
R.m.s. deviations from ideal value		
Bond lengths (Å)	0.011	0.011
Bond angles (°)	0.031	0.029
Zero chiral volumes (Å^3)	0.067	0.061
Distances from restrained planes (Å)	0.028	0.027
Mean B factors (Å^2)		
Overall	24.7	18.1
Main-chain atoms	24.8	18.3
FMN atoms	16.1	9.8
Side chain + solvent atoms	24.5	17.8

3. Material and methods

Bipyramidal yellow crystals of both the wt and S35C mutant grew from 3.2 *M* ammonium sulfate, 0.1 *M* Tris–HCl pH 7 with protein concentrations ranging between 6 and 8 mg ml^{-1}. Crystallization was carried out at room temperature (295 K) by the sitting-drop vapour-diffusion technique. Crystals of similar quality were obtained by the hanging-drop technique.

Cryogenic temperature (100 K) data were collected on the ELETTRA synchrotron beamline, Trieste, with an X-ray wavelength of 1 Å using a MAR image-plate scanner. The program *MOSFLM* was used for elaborating each frame and finding the space group; the programs *SORT* and *SCALA* (Collaborative Computational Project, Number 4, 1994) were used for indexing, processing and scaling the data.

High-resolution data to 1.34 Å were collected for wt flavodoxin at a crystal-to-detector distance of 180 mm with a 180° φ range and a φ increment of 1°; low-resolution data were collected at a crystal-to-detector distance of 250 mm using the same φ range. Data to 1.44 Å were collected using a similar procedure for the S35C mutant.

3.1. Structure refinement

A flavodoxin model in the same crystal form (PDB code 3fx2; Watt *et al.*, 1991) without solvent molecules was used as a starting point for refinement of the wt flavodoxin.

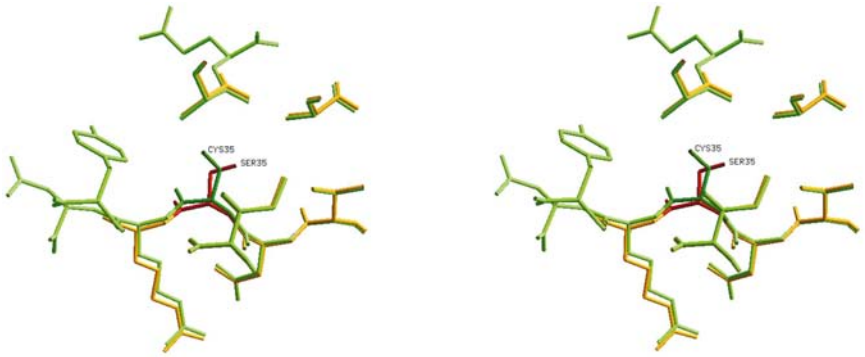

Figure 3
Stereoview of the superimposition of residues in a 5.0 Å radius around the mutation site in wt (red) and S35C (yellow) flavodoxins.

The refinement process utilized the program *SHELX*97 (Sheldrick, 1997) and its auxiliary program *SHELXPRO* for map calculation, updating structures files, data and model analysis. 5% of the reflections were set aside for cross-validation analysis by means of $R_{\rm free}$ (Brünger, 1993). Each step of refinement consisted of ten cycles of restrained conjugate-gradient-square minimization and, in every run, the output files were updated to input files with *SHELXPRO*. Bulk-solvent contributions were automatically calculated using Babinet's principle (Moews & Kretsinger, 1975). After every refinement job, the displacement parameters of the water molecules were examined and the $2F_o - F_c$ maps were analysed to find the highest peaks which involve no bad contacts and make geometrically plausible hydrogen bonds. These peaks were included with full occupancy and oxygen scattering factor in the next refinement job.

Protein bonds and angle restraints were those of Engh & Huber (1991). Anti-bumping distance restraints were added to prevent non-bonded collision. After three steps of refinements without solvent in the resolution interval 10.0–1.35 Å, R and $R_{\rm free}$ decreased to 32.5 and 35.6%, respectively. After each step, $2F_o - F_c$ electron-density maps were calculated and the model was rebuilt, if necessary, using the program *O* (Jones *et al.*, 1991; Jones & Kjeldgaard, 1993). After five jobs performed with isotropic refinement and bulk-solvent parameters, the calculated R and $R_{\rm free}$ were 25.6 and 30.1%, respectively. H atoms were included at the end of the isotropic refinement at calculated positions. Anisotropic B factors were introduced during the ninth round of refinement and R and $R_{\rm free}$ fell to values of 18.1 and 23.5%, respectively. Minor adjustments for better fitting of the model to the $2F_o - F_c$ electron-density map were made with the program *O*; R and $R_{\rm free}$ further decreased to 16.8 and 22.4%, respectively. At this point of refinement, we extended the resolution interval to infinite, changing the weighting scheme to 0.2, with anisotropic thermal factors for the water molecules. After two refinement cycles, convergence was reached with R and $R_{\rm free}$ of 15.8 and 17.9%, respectively. In the final wt flavodoxin model there are 147 amino acids, one molecule of FMN and 185 water molecules.

The model fits very well in the $2F_o - F_c$ electron-density map, except for the side chain of the last two protein residues (Ala147 and Ile148). The three-dimensional structure of oxidized flavodoxin at 100 K is essentially the same as that reported by Watt *et al.* (1991). However, the electron-density map calculated from the high-resolution data provides considerable detail and new structural information, especially in side-chain conformations. The accuracy of the model is confirmed from the low r.m.s. deviations from ideal values, *i.e.* for bond lengths (0.01 Å) and angle distances (0.03 Å). Analysis of the stereochemistry of the model using *PROCHECK* (Laskowski *et al.*, 1993) shows that all geometric parameters are within the limit expected for this resolution. The Ramachandran plot (Ramachandran & Sasisekharan, 1968) shows only one residue, Asp62, in a disallowed region. However, this residue is well defined in the electron-density map.

This model was then used as a starting point for the refinement of S35C with *SHELX*97. The procedure for the refinement was the same as with wt. The final model, based on 109 cycles of *SHELXL*97, data ranging from 16.37 to 1.44 Å, includes 174 water molecules and gives R and $R_{\rm free}$ values of 13.4 and 15.6%, respectively. A summary of the crystal data and refinement statistics is shown in Table 2.

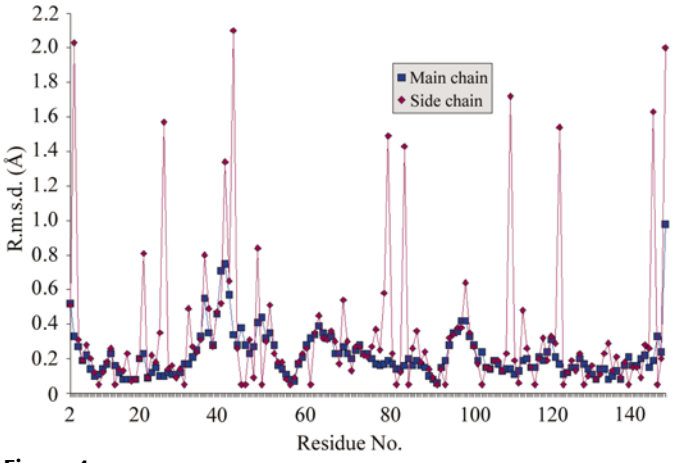

Figure 4
Plot of the r.m.s.d. between main-chain and side-chain atoms of wt and the mutant S35C.

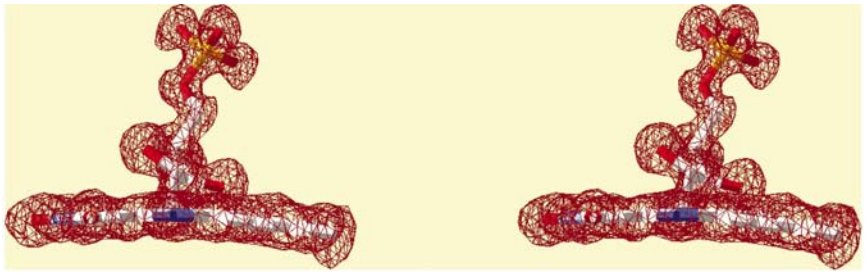

Figure 5
Stereoview of the $2F_o - F_c$ electron-density map (1.5σ) of the cofactor FMN in the S35C mutant.

We gratefully acknowledge Dr Alberto Cassetta and Dr Doriano Lamba for their skilful technical advice at the ELETTRA synchrotron facility and the Elettra Synchrotron Light Source (Trieste, Italy) for beamline access. Financial support from the Ministero dell'Università e della Ricerca Scientifica e Tecnologica (Italy) and the BBSRC (UK) are also acknowledged.

References

Brünger, A. T. (1993). *Acta Cryst.* D**49**, 24–36.
Burkhart, B. M., Ramakrishnan, B., Hongao, Y., Reedstron, R. J., Markley, J. L., Straus, N. A. & Sundaralingam, M. (1995). *Acta Cryst.* D**51**, 318–330.
Collaborative Computational Project, Number 4 (1994). *Acta Cryst.* D**50**, 760–763.

Drennan, C. L., Pattridge, K. A., Weber, C. H., Metzger, A. L., Hoover, D. M. & Ludwig, M. L. (1999). *J. Mol. Biol.* **294**, 711–724.
Engh, R. A. & Huber, R. (1991). *Acta Cryst.* A**47**, 392–400.
Freigang, J., Diederichs, K., Schafer, K. P., Welte, W. & Paul, R. (2002). *Protein Sci.* **11**, 253–61.
Fukuyama, K., Matsubara, H. & Rogers, L. J. (1992). *J. Mol. Biol.* **225**, 775–789.
Gilardi, G., Meharenna, Y. T., Tsotsou, G. E., Sadeghi, S. J., Fairhead, M. & Giannini, S. (2002). *Biosens. Bioelectron.* **17**, 133–145.
Hoover, D. M., Drennan, C. L., Metzger, A. L., Osborne, C., Weber, C. H., Pattridge, K. A. & Ludwig, M. L. (1999). *J. Mol. Biol.* **294**, 725–742.
Hoover, D. M. & Ludwig, M. L. (1997). *Protein Sci.* **12**, 2525–2537.
Jones, T. A. & Kjeldgaard, M. (1993). *O – The Manual*. Uppsala University, Uppsala, Sweden.
Jones, T. A., Zou, J.-Y., Cowan, S. W. & Kjeldgaard, M. (1991). *Acta Cryst.* A**47**, 110–119.
Laskowski, R. A., MacArthur, M. W., Moss, D. S. & Thornton, J. M. (1993). *J. Appl. Cryst.* **26**, 283–291.
Laudenbach, D. E., Straus, N. A., Pattridge, K. A. & Ludwig, M. L. (1987). *Flavins and Flavoproteins*, edited by D. E. Edmondson & D. B. McCormick, pp. 249–260. Berlin/New York: W. de Gruyter & Co.
Lennon, B. W., Williams, C. H. Jr & Ludwig, M. L (1999). *Protein Sci.* **8**, 2366–2379.
Ludwig, M. L., Burnett, R. M., Darling, G. D., Jordan, S. R., Kendall, D. S. & Smith, W. W. (1976). *Flavins and Flavoproteins*, edited by T. P. Singer, pp. 393–404. Amsterdam: Elsevier.
Ludwig, M. L. & Luschinsky, C. L. (1992). *Chemistry and Biochemistry of Flavoenzymes*, edited by F. Muller, Vol. 3, pp. 427–466. Boca Raton, FL, USA: CRC Press.
Ludwig, M. L., Pattridge, K. A., Metzger, A. L., Dixon, M. M., Eren, M., Feng, Y. & Swenson, R. P. (1997). *Biochemistry*, **36**, 1259–1280.
McDonald, I. K. & Thornton, J. M. (1994). *J. Mol. Biol.* **238**, 777–793.
Mierlo, C. P. M. van, Lijnzaad, P., Vervoort, J., Muller, F., Berendsen, H. J. C. & de Vlieg, J. (1990). *Eur. J. Biochem.* **194**, 185–198.
Moews, P. C. & Kretsinger, R. H. (1975). *J. Mol. Biol.* **91**, 201–225.
Nagano, N., Ota, M. & Nishikawa, K. (1999). *FEBS Lett.* **458**, 69–71.
Ramachandran, G. & Sasisekharan, V. (1968). *Adv. Protein Chem.* **23**, 283–437.
Reynolds, R. A., Watt, W. & Watenpaugh, K. D. (2001). *Acta Cryst.* D**57**, 527–535.
Romero, A., Caldeira, J., Legall, J., Moura, I., Moura, J. J. & Romao, M. J. (1996). *Eur. J. Biochem.* **239**, 190–196.
Sadeghi, S. J., Meharenna, Y. T., Fantuzzi, A., Valetti, F. & Gilardi, G. (2000). *Faraday Discuss.* **116**, 135–153.
Sadeghi, S. J., Meharenna, Y. T. & Gilardi, G. (1999). *Flavins and Flavoproteins*, edited by S. Ghisla, P. Kroneck, P. Macheroux & H. Sund, pp. 125–129. Berlin: Agency for Scientific Publications.
Sadeghi, S., Valetti, F., Cunha, C. A., Romao, M. J., Soares, C. M. & Gilardi, G. (2000). *J. Biol. Inorg. Chem.* **5**, 730–737.
Sheldrick, G. M. (1997). *SHELX97. Program For The Refinement Of Crystal Structure.* University of Göttingen, Germany.
Smillie, R. M. (1965). *Biochem. Biophys. Res. Commun.* **20**, 621–629.
Smith, W. W., Pattridge, K. A., Ludwig, M. L., Petsko, G. A., Tsernoglou, D., Tanaka, M. & Yasunobu, K. T. (1983). *J. Mol. Biol.* **165**, 737–753.
Valetti, F., Sadeghi, S. J., Meharenna, Y. & Gilardi, G. (1998). *Biosens. Bioelectron.* **13**, 675–685.
Wallace, A. C., Laskowski, R. A. & Thornton, J. M. (1995). *Protein Eng.* **8**, 127–134.
Walsh, M. A., McCarthy, A., O'Farrell, P. A., McArdle, P., Cunningham, P. D., Mayhew, S. G. & Higgins, T. M. (1998). *Eur. J. Biochem.* **258**, 362–371.
Watt, W., Tulinski, A., Swenson, R. P. & Watenpaugh, K. D. (1991). *J. Mol. Biol.* **218**, 195–208.